www.nature.com/aps

Acta Pharmacologica Sinica

ARTICLE

Deubiquitinating enzyme USP11 promotes renal tubular cell senescence and fibrosis via inhibiting the ubiquitin degradation of TGF-β receptor II

Jia-yun Ni[1], Xin Wang[1], Hong-yan Xie[1], Ning-hao Yang[1], Jing-yao Li[1], Xi-ang Sun[1], Heng-jiang Guo[1], Li Zhou[1], Wei Zhang[1], Jun Liu[1] and Li-min Lu[1,2]

Transforming growth factor-β1 (TGF-β1) is regarded as a key factor in promoting renal fibrosis during chronic kidney disease (CKD). Signaling transduction of TGF-β1 starts with binding to TGF-β type II receptor (Tgfbr2), a constitutively activated kinase that phosphorylates TGF-β type I receptor (Tgfbr1), and then activates downstream Smad2/3 or noncanonical pathways. Previous studies show that cellular senescence is associated with the progression of CKD, and accelerated tubular cell senescence is implicated in promoting renal fibrosis. In the present study we investigated the renal parenchymal cell senescence in fibrosis from the sight of posttranslational regulation and focused on Tgfbr2, the important gatekeeper for TGF-β1 downstream signaling. In mice with unilateral ureteral obstruction (UUO) and folic acid (FA)-induced fibrotic kidneys, we found that Tgfbr2 was markedly elevated without obvious change in its mRNA levels. As an important member of deubiquitinating enzymes, ubiquitin-specific protease 11 (Usp11) was also significantly increased in fibrotic kidneys, and co-distributed with Tgfbr2 in tubular epithelial cells. Pretreatment with Usp11 inhibitor mitoxantrone (MTX, 30 mg · kg^{-1} · d^{-1}, i.p.) twice a week, for 2 weeks significantly attenuated the elevation of Tgfbr2, activation in downstream senescence-related signaling pathway, as well as renal senescence and fibrosis. In cultured mouse tubular epithelial cells (MTECs), treatment with angiotensin II (Ang-II, 10^{-7}, 10^{-6} M) dose-dependently elevated both Tgfbr2 and Usp11 levels. Inhibition or knockdown on Usp11 attenuated Ang-II-induced elevation in Tgfbr2 level, and attenuated the activation of downstream senescent-related signaling pathway and as well as cell senescence. We conducted Co-IP experiments, which revealed that Usp11 was able to interact with Tgfbr2, and inhibition of Usp11 increased the ubiquitination of Tgfbr2. Taken together, these results demonstrate that the elevation of Usp11 under pathological condition is implicated in promoting renal fibrosis. Usp11 promotes the development of renal fibrosis by deubiquitinating Tgfbr2, reducing Tgfbr2 ubiquitination degradation, and then facilitating the activation of downstream senescent signaling pathway.

Keywords: renal fibrosis; renal tubular epithelial cell; cellular senescence; TGF-β1; Tgfbr2; Usp11

Acta Pharmacologica Sinica (2023) 44:584–595; https://doi.org/10.1038/s41401-022-00977-5

INTRODUCTION

Chronic kidney disease (CKD) is currently considered as a worldwide health concern and a major threat to human health [1, 2]. Any kind of CKD is characterized by renal fibrosis whatever the original pathogenies, and will inevitably progress into the end-stage renal disease if no appropriate intervention is taken. Renal fibrosis is a consequence of disturbed extracellular matrix protein production and degradation, which leads to excessive sedimentation of extracellular matrix in renal interstitium and loss of renal parenchyma cells [3, 4]. Evidences from different studies have revealed that renal fibrosis is not only a morphological characteristic, but also an independent risk for the development of CKD.

Renal fibrosis can be induced by various factors such as hypoxia, oxidative stress, growth hormones, and inflammatory cytokines. Among them, TGF-β1 is widely accepted as the most important fibrogenic initiator, which mediates the fibrotic effects of different factors, such as inflammatory factors, Ang-II, endothelin 1, ischemia, high glucose etc [5].

TGF-β1 exerts its biological effects via binding to TGF-β1 receptor on the cell membrane. TGF-β1 receptor is a heterodimer of subunits TGF-β type I receptor (Tgfbr1) and II (Tgfbr2). Tgfbr2 is the subunit that recognizing TGF-β1 in extracellular fluid. When Tgfbr2 binds with TGF-β1, it recruits and phosphorylates Tgfbr1 and then activates downstream canonical (Smad-dependent) and non-canonical (non-Smad-dependent) intracellular signaling pathways. The fibrosis-facilitating effects of TGF-β1 depend on the change of TGF-β1 expression as well as the sequential activation of its downstream signaling. Compared with the change of TGF-β1 expression, the regulations on each downstream signaling molecule under pathological situations are far from elucidated [6–8].

[1]Department of Physiology and Pathophysiology, School of Basic Medical Sciences, Fudan University, Shanghai 200032, China and [2]Shanghai Key Laboratory of Kidney and Blood Purification, Shanghai 200032, China
Correspondence: Jun Liu (junliu@shmu.edu.cn) or Li-min Lu (lulimin@shmu.edu.cn)
These authors contributed equally: Jia-yun Ni, Xin Wang

Received: 16 May 2022 Accepted: 7 August 2022
Published online: 31 August 2022

In the TGF-β1 downstream signaling pathway, the stability of multiple molecules can be regulated by different ways, including the ubiquitin-proteasome system (UPS) [9–12]. UPS is the major intracellular and non-lysosomal protein degradation system. It includes substrates, ubiquitin molecule, ubiquitin-activating enzymes (E1), ubiquitin-conjugating enzymes (E2), ubiquitin-ligase enzymes (E3), 26S proteasomes, and Deubiquitinating enzymes (DUB) [12–14]. DUBs are the enzymes which cleave ubiquitin from proteins and other molecules by hydrolyzing the ester bond, peptide bond, or iso-peptide bond at the carboxyl terminus of ubiquitin, thus negatively regulate ubiquitination-mediated protein degradation [14–16]. Usp11 belongs to the ubiquitin-specific protease enzyme subfamily in DUB [17]. It has been observed that Usp11 can control the ubiquitination of Tgfbr2 and was involved in the progression of pulmonary fibrosis [18].

Cellular senescence refers to the phenomenon that the cell loses duplicating ability and permanently exits cell cycle following repeatedly duplication [19–21]. Cellular senescence is the basis of ageing in multicellular organisms, but unlike ageing, cellular senescence is a physiological phenomenon which runs through entire lifetime of the organism. Different from quiescent cells, senescent cells cannot re-enter the cell cycle when subjected to stimuli, thus it will ultimately affect the functions of an organ. Senescent cells are characterized by morphological changes, chromatin remodeling, altered gene expression profile, and the appearance of senescence-associated secretory phenotype (SASP) [22]. Under pathological conditions, such as stress, the accelerated cellular senescence may lead to insufficiency in parenchymal cells, and is considered as a reason for pathological remodeling and functional deterioration of the organs. Thus, revealing the mechanism of accelerated cellular senescence under pathological conditions is considered as a new window for exploring effective manipulating strategy for degenerative diseases [23]. Previous studies have observed that cellular senescence is associated with the progression of CKD, and the accelerated tubular cell senescence is implicated in promoting renal fibrosis [24, 25].

In the present study, we aimed to investigate the mechanism of renal parenchymal cell senescence in fibrosis from the sight of posttranslational regulation and focused on the gatekeeper for TGF-β1 downstream signaling Tgfbr2.

MATERIALS AND METHODS

Animal models

Male C57BL/6J mice (6–8 weeks old, 20–25 g in bodyweight) were purchased from Animal Department of Fudan University (Shanghai, China). UUO mice were established as previously described [26]. After the mice were anesthetized, the left ureter was exposed and ligated. The sham group was operated in the same procedure except the left ureter ligation. Mice were administered with either saline or Usp11 inhibitor mitoxantrone (MTX) (MedChemExpress, Monmouth Junction, NJ, USA) via the intraperitoneal injection at a dose of 3 mg/kg bodyweight 2 weeks before UUO surgery, twice a week [27–29]. At 14 days, the mice were euthanized for the renal tissue harvesting. Folic acid (FA) mice received a single intraperitoneal injection of FA (250 mg/kg bodyweight; Sigma; Saint Louis, MO, USA) dissolved in a 0.3 M sodium bicarbonate solution and were euthanized at 21 days for the renal tissue harvesting. All animal experiments were conducted following the Guidance for Care and Use of Laboratory Animals of Fudan University. The protocols complied with the Criteria of the Medical Laboratory Animal Administrative Committee of Shanghai and were approved by the Ethics Committee for Experimental Research of Shanghai Medical College, Fudan University.

Cell culture

The mouse renal proximal tubular epithelial cell line (MTECs) was obtained from Prof. Lan's lab, Chinese University of Hong Kong. The cells were cultured in DMEM-F-12 medium (Cytiva; Logan, UT, USA) supplemented with 10% FBS (Gibco; Grand Island, NY, USA) and 1% penicillin–streptomycin (Gibco; Grand Island, NY, USA) in a humidified incubator with 5% CO_2 at 37 °C. After starved overnight in a serum-free medium, cells were treated with Ang-II (Millipore; Billerica, MA, USA) at a concentration of 10^{-7} and 10^{-6} M for 48 h. Usp11 inhibitor MTX (2.5 μmol/L) was added to cells for 0.5 h after Ang-II treatment.

Western blot

Kidney tissue or cells were lysed in lysis buffer containing 2% SDS following centrifugation. The supernatant was separated on SDS-polyacrylamide gels and then electrophoretically transferred to polyvinylidene fluoride membrane (Millipore; Billerica, MA, USA). The membrane was blocked with 5% non-fat milk for 2 h. Proteins were detected with primary antibody against Fibronectin (F3648; Sigma-Aldrich; Saint Louis, MO, USA), α-smooth muscle actin (α-SMA) (14395-1-Ig; Proteintech; Chicago, MA, USA), glyceraldehyde-3-phosphate dehydrogenase (GAPDH) (60004-1-Ig; Proteintech; Chicago, MA, USA), Tgfbr2 (66636-1-Ig; Proteintech; Chicago, MA, USA), Usp11 (ab109232; Abcam; Cambridge, MA, USA), Klotho (AF1819; R&D Systems; Minneapolis, MN, USA), γ-H2AX (9718S; Cell Signaling Technology; Beverly, MA, USA), P53 (2524S; Cell Signaling Technology; Beverly, MA, USA), P21 (sc-6246; Santa Cruz Biotechnology; Santa Cruz, CA, USA), P16 (ab51243; Abcam; Cambridge, MA, USA), p-Smad3 (9520S; Cell Signaling Technology; Beverly, MA, USA), Smad3 (9513S; Cell Signaling Technology; Beverly, MA, USA), ubiquitin (10201-2-AP; Proteintech; Chicago, MA, USA). The bands were visualized by an ECL detection kit and quantitated by densitometric analysis using the ImageJ software.

RNA extraction and real-time quantitative PCR

Total RNA was extracted using the TRIzol reagent (Thermo Fisher Scientific; Waltham, MA, USA). For mRNA quantification, cDNA was synthesized using PrimeScript™ RT reagent Kit (Takara; Kyoto, Japan) and quantitative PCR was performed on Applied Biosystems 7300 Plus using SYBR Green PCR master mix (Toyobo; Osaka, Japan). The sequences of the primer pairs are: 5′-CGTTTCCGGGACCAGAATCC-3′ (forward) and 5′-CATCGCCGTCCGTTCTCTTC-3′ (reverse) for Usp11; 5′-ACGTTCCCAAGTCGGATGTG-3′ (forward) and 5′-ACAGCTTAGGTGGATGGATGC-3′ (reverse) for Tgfbr2; 5′-CTTTGGTATCGTGGAAGGACTC-3′ (forward) and 5′-AGTAGAGGCAGGGATGATGT-3′ (reverse) for GAPDH. The relative abundance of target mRNA was normalized to the GAPDH.

Renal histology and immunohistochemistry staining

Mouse kidneys fixed in 10% formalin were embedded into paraffin and cut into 4-μm thick sections. H&E staining, Masson's trichrome staining and Sirius Red staining were conducted following a protocol described previously. The tubular injury was assessed by H&E staining based on tubular changes including tubule dilation, epithelial swelling, loss of brush borders, and protein cast formation. Masson's trichrome staining and Sirius Red staining were used to evaluate interstitial fibrosis. Fibrotic areas in five discretionary fields of each mouse were quantified. The average percentage of fibrotic area relative to the total area was regarded as fibrotic score. The mouse kidneys were stained using specific anti-Usp11 antibody (ab109232; Abcam; Cambridge, MA, USA) and anti-Tgfbr2 antibody (66636-1-Ig; Proteintech; Chicago, MA, USA).

RNA interference

Usp11 siRNA (5′-UUAUCUCAUCUUGAAAGAGUG-3′) was designed and synthesized by Biotend (Shanghai, China). MTECs were transfected with Usp11 siRNA (25 μmol/L) or non-silencing negative siRNA (25 μmol/L) using Lipofectamine RNAiMAX reagent (13778030; Thermo Fisher Scientific; Waltham, MA, USA) according to the manufacturer's instructions.

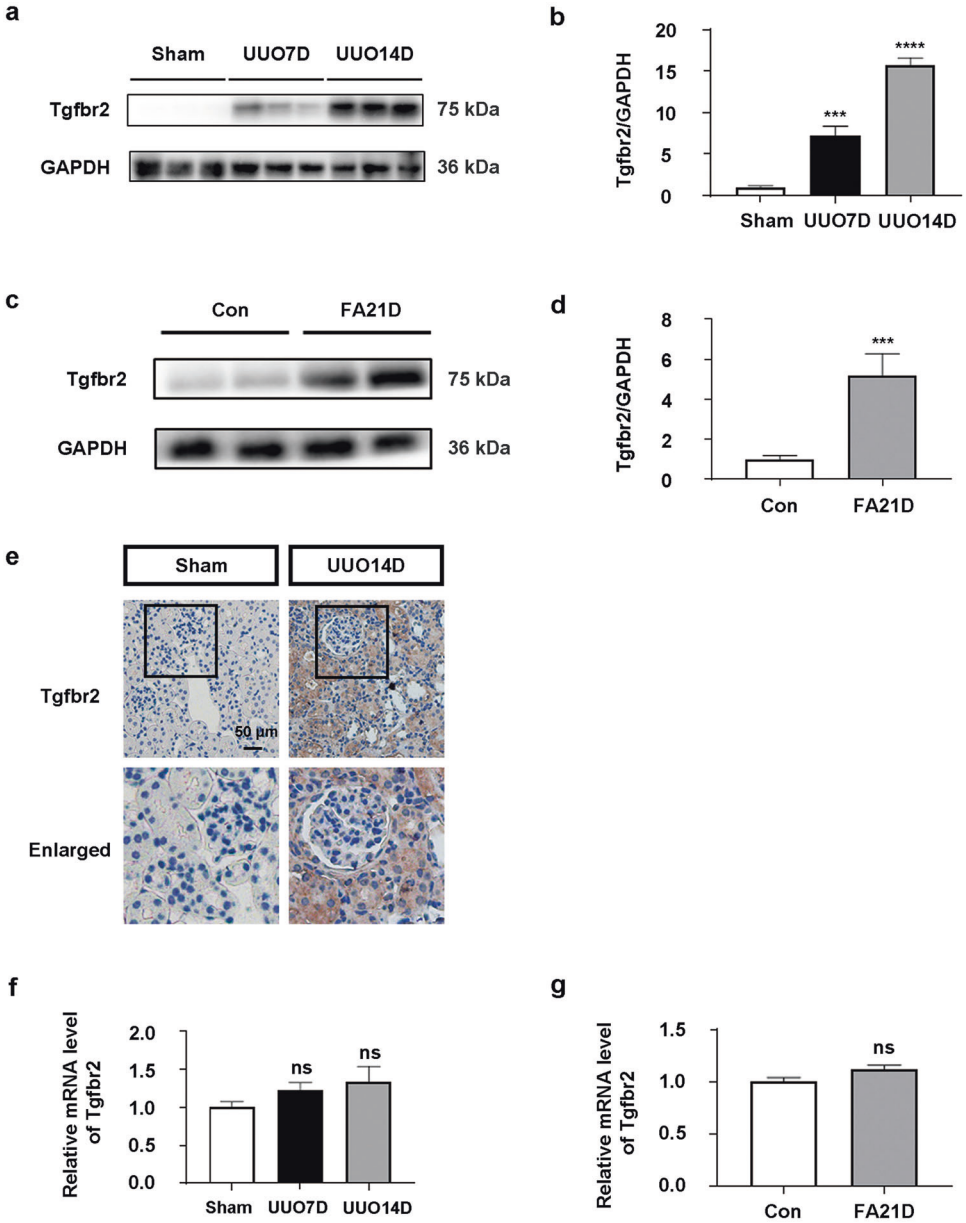

Fig. 1 The Tgfbr2 protein level but not mRNA level was elevated in tubular epithelial cells in UUO or FA-induced fibrotic kidneys. **a** Representative Western blot of Tgfbr2 in UUO mice kidneys. **b** Quantitative data for Tgfbr2 in mice kidneys at 7 and 14 d after UUO ($n = 6$). ***$P < 0.001$, ****$P < 0.0001$ vs Sham. **c** Representative Western blot of Tgfbr2 in FA mice kidneys. **d** Quantitative data for Tgfbr2 in mice kidneys at 21 d after FA treatment ($n = 6$). ***$P < 0.001$ vs *Con*. **e** Immunohistochemistry staining of Tgfbr2 in sham and UUO mice at 14 d after surgery. Scale bars: 50 μm. **f** qPCR analysis for Tgfbr2 mRNA in the kidneys at 7 d, 14 d after UUO ($n = 6$). Ns, $P > 0.05$ vs Sham. **g** qPCR analysis for Tgfbr2 mRNA in the kidneys at 21 d after FA ($n = 6$). Ns, $P > 0.05$ vs Con. Con control, FA folic acid, UUO unilateral ureteral obstruction.

Coimmunoprecipitation (Co-IP)

Cells were lysed in a mild cell lysate (P0013; Beyotime; Shanghai, China). After centrifugation at 14,000 × *g* for 10 min at 4 °C, the supernatants were incubated with anti-Usp11 (ab109232; Abcam; Cambridge, MA, USA) or anti-Tgfbr2 (66636-1-Ig; Proteintech; Chicago, MA, USA) overnight at 4 °C and then precipitated by the Protein A/G PLUS-Agarose (Santa Cruz, Dallas, TX, USA). The IP complexes were washed and eluted for immunoblot analysis.

Senescence-associated β-galactosidase (SA-β-gal) staining

Frozen sections (3 μm) were used for detection of SA-β-gal activity according to the manufacturer's instructions (C0602; Beyotime; Shanghai, China).

Statistical analysis

Data are shown as the mean ± SEM. The analysis of data was performed by SPSS 19.0 (Chicago, IL, USA). Comparisons among groups were performed by one-way ANOVA with post hoc analysis using Tukey's test. $P < 0.05$ was considered as statistically significant.

RESULTS

Tgfbr2 was increased in UUO or FA-induced fibrotic kidneys

Western blot result showed that Tgfbr2 was significantly increased in the obstructed kidneys of UUO mice compared with sham-operated mice (Fig. 1a, b). The elevation of Tgfbr2 was also observed in FA-induced renal fibrosis animals (Fig. 1c, d).

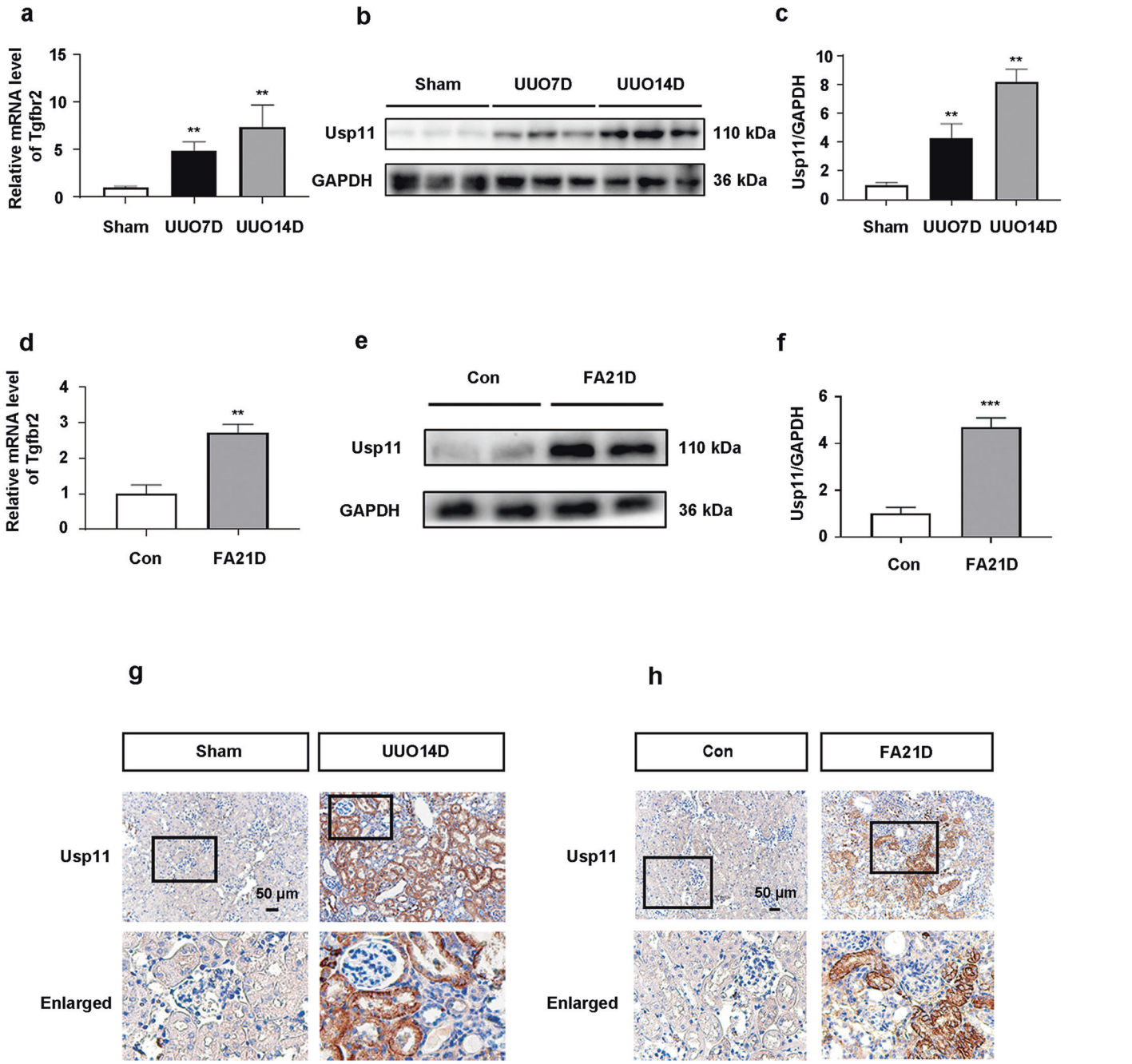

Fig. 2 Usp11 was elevated in tubular epithelial cells in UUO or FA-induced fibrotic kidneys. **a** qPCR analysis for Usp11 mRNA in the kidneys at 7 d, 14 d after UUO ($n = 6$). $^{**}P < 0.01$ vs Sham. **b** Representative Western blot of Usp11 in UUO mice kidneys. **c** Quantitative data for Usp11 in mice kidneys at 7 and 14 d after UUO ($n = 6$). $^{**}P < 0.01$ vs Sham. **d** qPCR analysis for Usp11 mRNA in the kidneys at 21 d after FA ($n = 6$). $^{**}P < 0.01$ vs Con. **e** Representative Western blot of Usp11 in FA mice kidneys. **f** Quantitative data for Usp11 in mice kidneys at 21 d after FA treatment ($n = 6$). $^{***}P < 0.001$ vs Con. **g** Immunohistochemistry staining of Usp11 in sham and UUO mice at 14 d after surgery. Scale bars: 50 μm. **h** Immunohistochemistry staining of Usp11 in Sham and FA mice at 21d after surgery. Scale bars: 50 μm. Con control, FA folic acid, UUO unilateral ureteral obstruction.

Immunohistochemistry result showed that Tgfbr2 was mainly distributed in renal tubules (Fig. 1e). The changes of Tgfbr2 in the obstructed kidneys were also measured by qPCR, however, the result showed that there was no significant difference in the mRNA levels of Tgfbr2 between UUO and Sham mice (Fig. 1f). In consistent with the qPCR results, also no significant difference in the mRNA level of Tgfbr2 was observed in FA mouse kidney tissue when compared with control mice (Fig. 1g).

Usp11 was increased in UUO or FA-induced fibrotic kidneys

Previous studies have demonstrated that deubiquitinating enzyme Usp11 reduces Tgfbr2 degradation by deubiquitination modification. Here, the expression of Usp11 in fibrotic mice was detected by Western blot and qPCR. The results showed that both Usp11 mRNA and protein levels were significantly increased in the obstructed kidneys of UUO mice compared with sham-operated mice (Fig. 2a–c). The elevation of Usp11 was also observed in FA-induced renal fibrosis animals (Fig. 2d–f). Immunohistochemistry

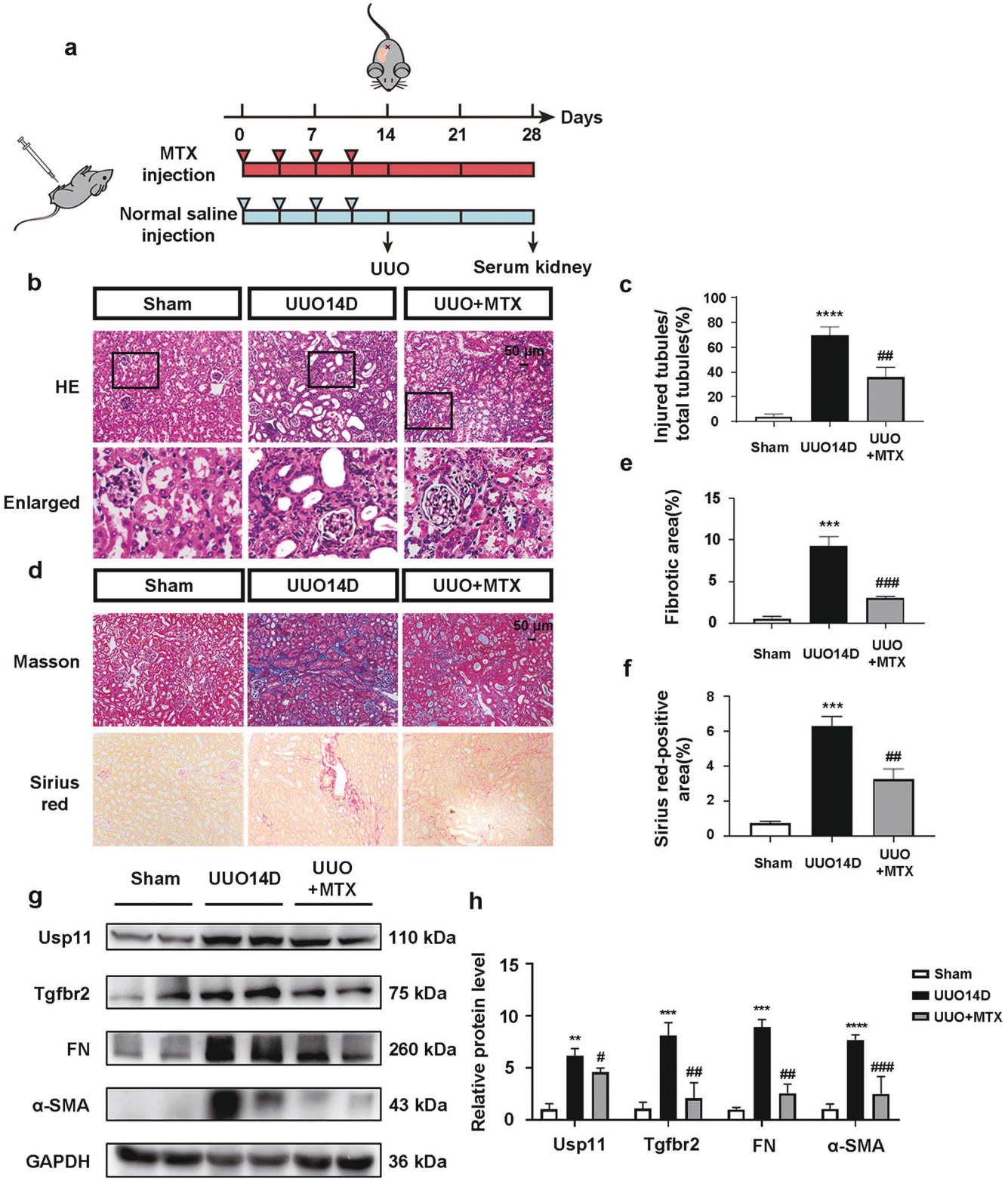

Fig. 3 Usp11 inhibitor mitoxantrone alleviated the elevation of Tgfbr2 and fibrotic-related gene expressions in UUO mice. a Experimental design. The blue arrowheads indicate the injections of MTX (3 mg/kg body weight), whereas the red arrowheads indicate the injections of vehicle (saline). **b** Representative H&E stained kidney images. Scale bars: 50 μm. **c** Quantitative determination of tubular injury score ($n = 6$). $^{****}P < 0.0001$ vs Sham. $^{\#\#}P < 0.01$ vs UUO. **d** Representative Masson and Sirius red staining kidney images. Scale bars: 50 μm. **e** Assessment of interstitial fibrosis based on Masson staining ($n = 6$). $^{***}P < 0.001$ vs Sham. $^{\#\#\#}P < 0.001$ vs UUO. **f** Quantitative determination of Sirius red positive area. $^{***}P < 0.001$ vs Sham. $^{\#\#}P < 0.01$ vs UUO. **g** Representative Western blot. **h** Quantitative data of Usp11, Tgfbr2, fibronectin and α-SMA from different groups ($n = 6$). $^{**}P < 0.01$, $^{***}P < 0.001$, $^{****}P < 0.0001$ vs Sham. $^{\#}P < 0.05$, $^{\#\#}P < 0.01$, $^{\#\#\#}P < 0.001$ vs UUO. FN fibronectin, H&E hematoxylin-eosin, Masson Masson's trichrome, MTX mitoxantrone, UUO unilateral ureteral obstruction, α-SMA α-smooth muscle actin.

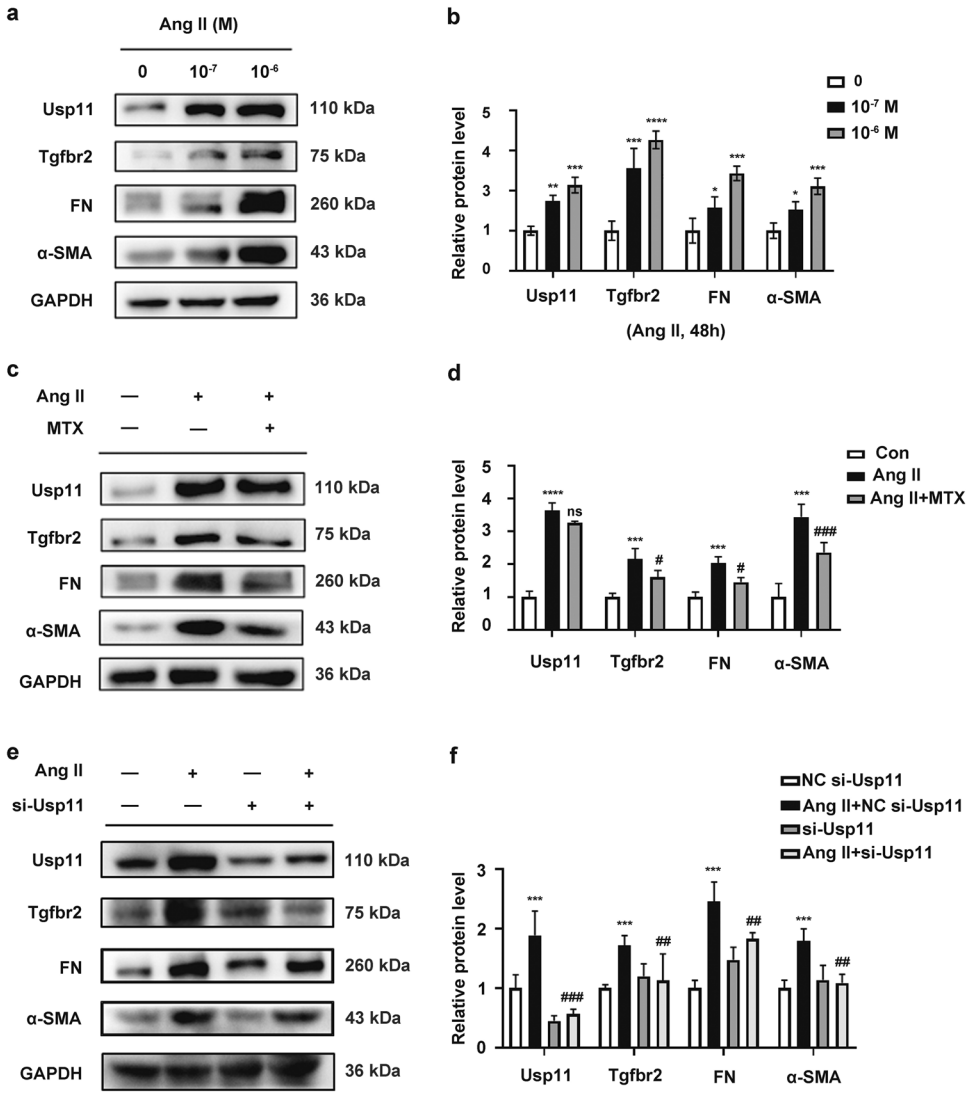

Fig. 4 Suppression of Usp11 attenuated Ang-II-induced the expressions of Tgfbr2 and fibrosis-related genes in MTECs. a Representative Western blot of Usp11, Tgfbr2, and fibrosis-associated genes. Cells were treated with Ang-II at a concentration of 10^{-7} and 10^{-6} M for 48 h. **b** Quantitative data for Usp11, Tgfbr2 and fibrosis-associated genes after Ang-II treatment ($n = 3$). $^{*}P < 0.05$, $^{**}P < 0.01$, $^{***}P < 0.001$, $^{****}P < 0.0001$ vs Con. **c** Representative Western blot of Usp11, Tgfbr2 and fibrosis-associated genes. Cells were pre-treated with Ang-II (10^{-6} M) for 48 h and then treated with MTX for 0.5 h. **d** Quantitative data for Usp11, Tgfbr2 and fibrosis-associated genes after Ang-II and MTX treatment ($n = 3$). $^{***}P < 0.001$, $^{****}P < 0.0001$ vs Con. Ns, $P > 0.05$, $^{\#}P < 0.05$, $^{\#\#\#}P < 0.001$ vs Ang-II. **e** Representative Western blot of Usp11, Tgfbr2 and fibrosis-associated genes. Cells were pre-treated with Usp11 siRNA (25 μmol/L) or NC siRNA (25 μmol/L) for 24 h and then exposed to Ang-II (10^{-6} M) for 48 h. **f** Quantitative data for Usp11, Tgfbr2 and fibrosis-associated genes after siRNA and Ang-II treatment ($n = 3$). $^{***}P < 0.001$ vs NC si-Usp11. $^{\#\#}P < 0.01$, $^{\#\#\#}P < 0.001$ vs Ang-II + NC si-Usp11. Con control, FN fibronectin, MTX mitoxantrone, α-SMA α-smooth muscle actin, MTEC mouse tubular epithelial cell.

result showed that Usp11 was mainly distributed in renal tubules (Fig. 2g, h).

Usp11 inhibitor MTX significantly enhanced the degradation of Tgfbr2 and alleviated fibrosis

To identify the role of Usp11 on renal fibrosis, MTX, an Usp11 inhibitor, was injected intraperitoneally into UUO mice (Fig. 3a). The obstructed kidneys displayed typical fibrosis characteristics, which was evidenced as the loss of brush border, tubule dilatation and cast formation by H&E staining analysis and extra interstitial extracellular matrix deposition by Sirius Red staining and Masson staining analysis. Inhibition of Usp11 by MTX significantly alleviated the pathological changes in obstructed kidneys (Fig. 3b–f). Western blot result revealed that the expression of Usp11 and Tgfbr2 were significantly increased in the obstructed kidneys. In addition, the expression of extracellular matrix component FN and renal fibrosis maker α-SMA was significantly increased in the obstructed kidneys. Administration of MTX effectively attenuated UUO-induced activation of Usp11 and Tgfbr2. In the same time, the elevations of FN and α-SMA were also significantly blunted (Fig. 3g, h).

Suppression of Usp11 blunted Ang-II-induced the Tgfbr2 expression and related gene expressions in MTECs

To verify the result observed in vivo, cultured renal tubular epithelial cells were treated with Ang-II, the major effector in renin-angiotensin system. As shown in Fig. 4a, b, Ang-II induced significant increases in Usp11 and Tgfbr2 expression in a dose-dependent manner, as well as the extracellular matrix component fibronectin and renal fibrosis maker α-SMA. Western blot results showed that pharmacological inhibition of Usp11 by MTX alleviated Ang-II-induced upregulation in Tgfbr2 and fibrosis-related genes

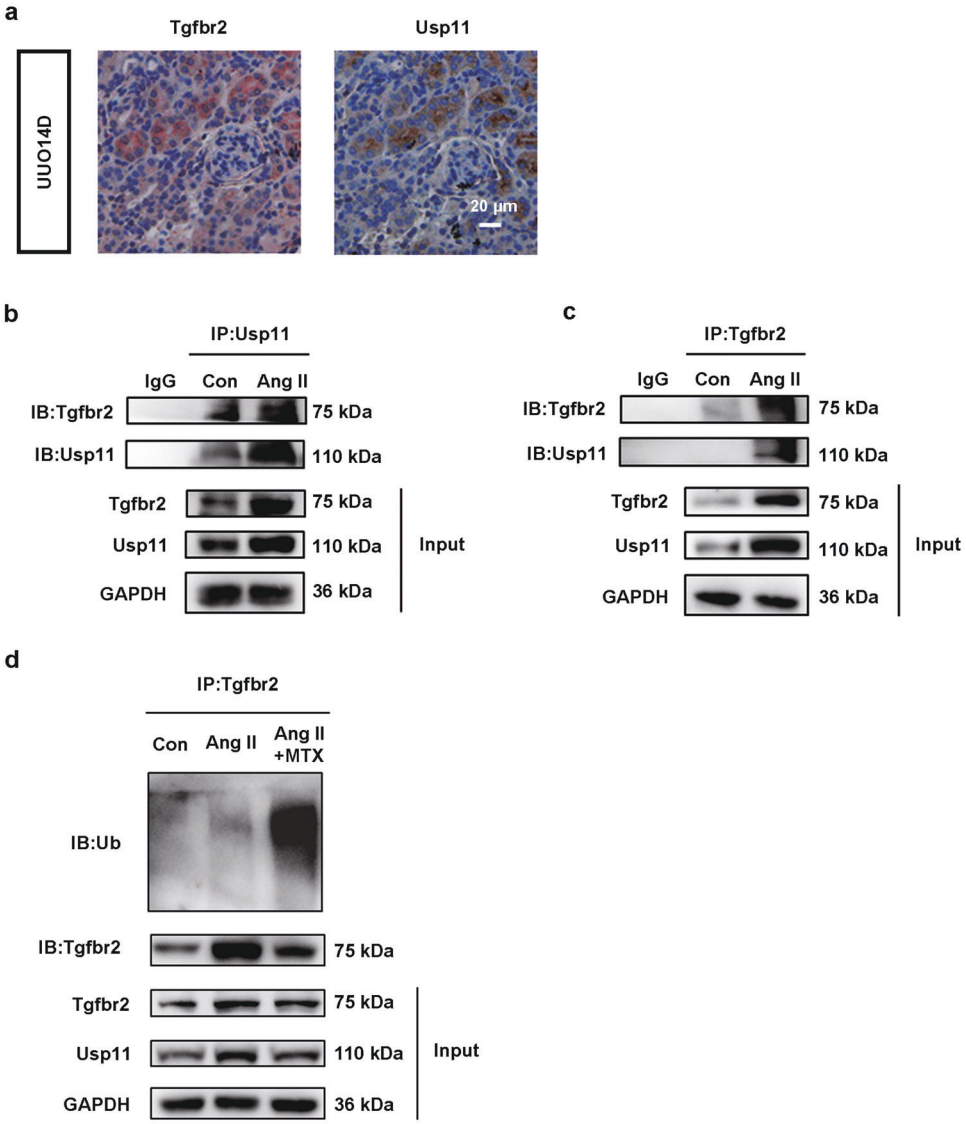

Fig. 5 Usp11 decreased the ubiquitination of Tgfbr2. a Representative immunohistochemistry staining images of co-localization of Usp11 and Tgfbr2 in UUO kidneys. Scale bars: 20 μm. **b** Mice tubular epithelial cells were treated with Ang-II for 48 h. Cell lysates were immunoprecipitated with anti-Usp11 antibody and analyzed by immunoblotting with anti-Tgfbr2 antibody. **c** Mice tubular epithelial cells were treated with Ang-II for 48 h. Cell lysates were immunoprecipitated with anti-Tgfbr2 antibody and analyzed by immunoblotting with anti-Usp11antibody. **d** Cells were pre-treated with Ang-II (10^{-6} M) for 48 h and then treated with MTX for 0.5 h. Cell lysates were immunoprecipitated with anti-Tgfbr2 antibody and analyzed by immunoblotting with anti-Ubiquitin antibody. Con control, MTX mitoxantrone, Ub Ubiquitin, UUO unilateral ureteral obstruction.

such as FN and α-SMA. However, MTX treatment had little effect on the expression of USP11 (Fig. 4c, d). In the same time, Western blot results showed that knockdown on Usp11 markedly reversed the increase of Usp11 induced by Ang-II in MTECs. Meanwhile, the increase of Tgfbr2 was attenuated by knockdown on Usp11. Ang-II-induced increases in FN and α-SMA were also reversed by knockdown on Usp11 (Fig. 4e, f). These results suggested that Usp11 was implicated in Ang-II-induced Tgfbr2 expression in renal epithelial cells.

Usp11 decreased the ubiquitination of Tgfbr2

Co-localization of Usp11 and Tgfbr2 was identified by IHC staining on serial sections of kidney. The results showed that the elevation of Usp11 protein was co-localized with Tgfbr2 in renal tubular epithelial cells of UUO kidneys (Fig. 5a). Co-IP was further conducted to verify the interaction between Usp11 and Tgfbr2. The results showed that Usp11 was able to interact with Tgfbr2 (Fig. 5b, c). Meanwhile, the results showed that MTX notably reduced the expression of Tgfbr2, while the number of Ubiquitin (Ub) molecules attached to Tgfbr2 was increased (Fig. 5d). These results suggested that the inhibition of Usp11 increased the ubiquitination of Tgfbr2.

Renal parenchymal cell senescence was exacerbated in UUO kidneys and Ang-II-treated MTECs

Cell senescence is considered as an accelerator of the functional deterioration of organs. In this study, Western blot result showed that the expressions of cell senescence markers, such as γH2AX, P53, and P21 were increased in UUO kidneys, while Klotho, an anti-aging factor, was downregulated (Fig. 6a–c). SA-β-gal staining showed that the SA-β-gal positive staining area was also increased in UUO kidneys (Fig. 6d, e). Similar results showed that the expression of senescence markers, such as γH2AX, P53, and P21, was increased in Ang-II-treated MTECs (Fig. 6f, g). Cell SA-β-gal

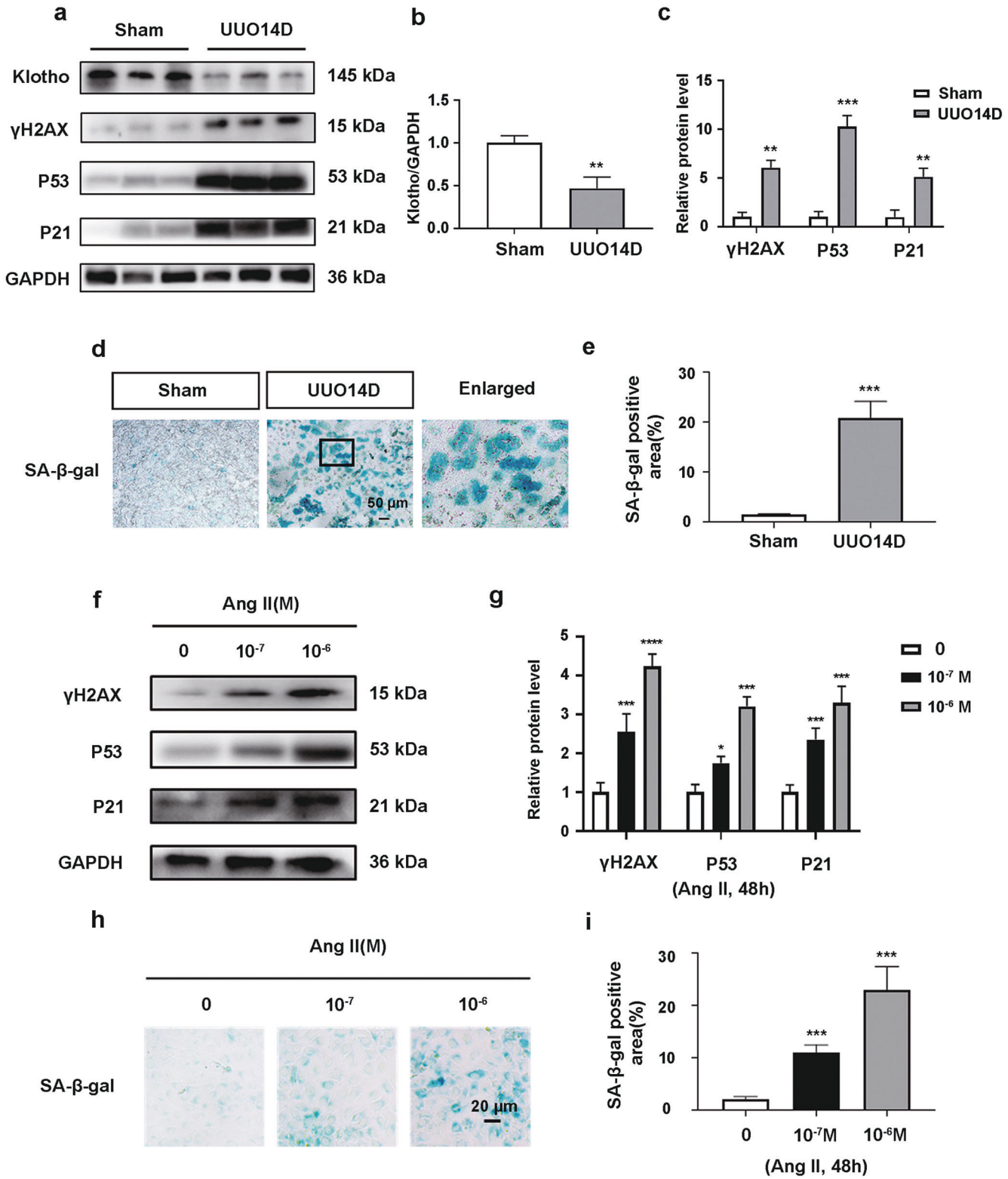

Fig. 6 Renal parenchymal cell senescence was exacerbated in UUO mice kidneys and Ang-II-treated MTECs. a Representative Western blot of cell senescence markers in UUO mice kidneys. **b**, **c** Quantitative data for cell senescence markers in UUO mice kidneys ($n = 6$). $^{**}P < 0.01$, $^{***}P < 0.001$ vs Sham. **d** Representative SA-β-gal staining images in sham and UUO mice at 14 d after surgery. Scale bars: 50 μm. **e** Quantitative determination of SA-β-gal positive area ($n = 6$). $^{***}P < 0.001$ vs Sham. **f** Representative Western blot of cell senescence markers. Cells were treated with Ang-II at a concentration of 10^{-7} and 10^{-6} M for 48 h. **g** Quantitative data for cell senescence markers after Ang-II treatment ($n = 3$). $^{*}P < 0.05$, $^{***}P < 0.001$, $^{****}P < 0.001$ vs Con. **h** Representative SA-β-gal staining Images. Cells were treated with Ang-II at a concentration of 10^{-7} and 10^{-6} M for 48 h. Scale bars: 20 μm. **i** Quantitative determination of SA-β-gal positive area ($n = 3$). $^{***}P < 0.001$ vs Con. Con control, SA-β-gal Senescence-associated β-galactosidase, UUO unilateral ureteral obstruction, MTEC mouse tubular epithelial cell.

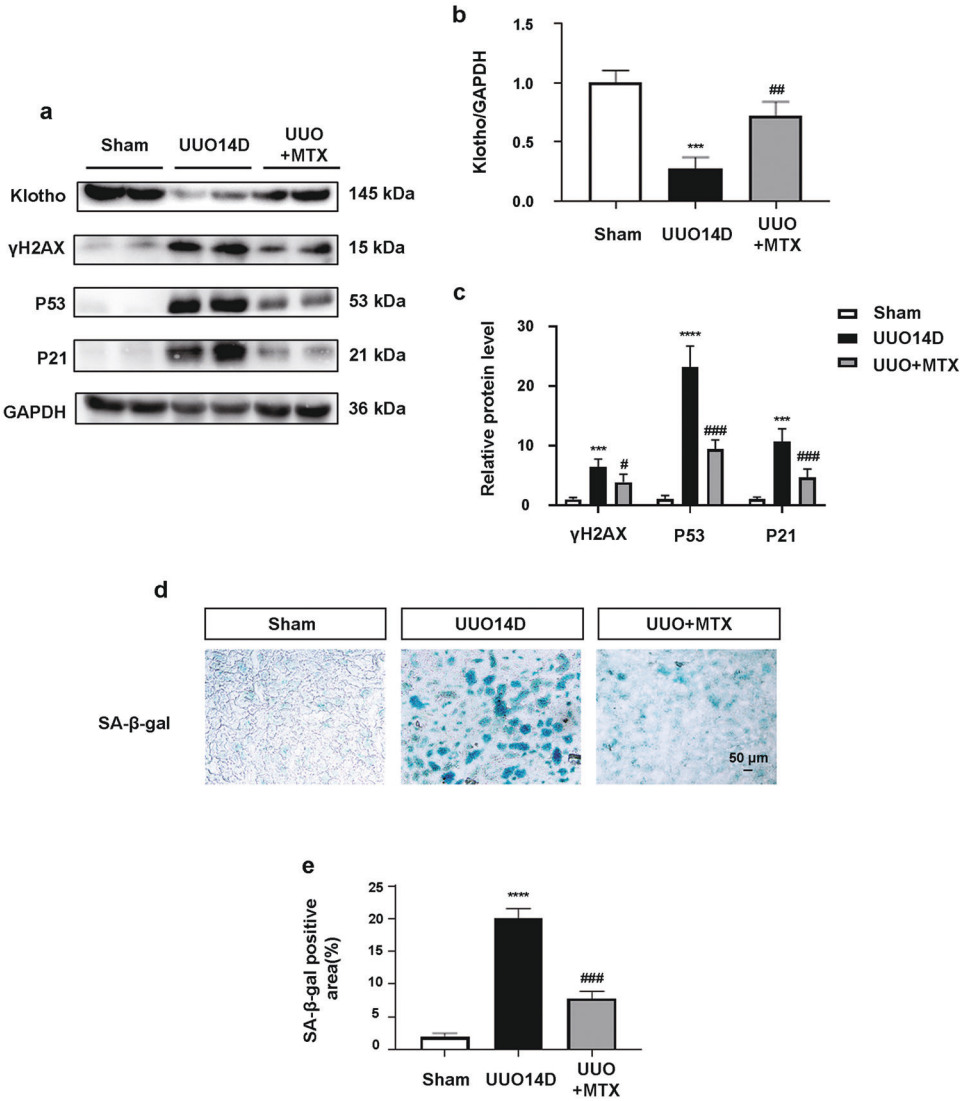

Fig. 7 Inhibition of Usp11 attenuated cell senescence in UUO mice kidneys. a Representative Western blot from different groups. **b**, **c** Quantitative data of cell senescence markers from different groups ($n = 6$). $^{***}P < 0.001$, $^{****}P < 0.0001$ vs Sham. $^{\#}P < 0.05$, $^{\#\#}P < 0.01$, $^{\#\#\#}P < 0.001$ vs UUO. **d** Representative SA-β-gal staining images from different groups. Scale bars: 50 μm. **e** Quantitative determination of SA-β-gal positive area ($n = 6$). $^{****}P < 0.0001$ vs Sham. $^{\#\#\#}P < 0.001$ vs UUO. MTX mitoxantrone, SA-β-gal Senescence-associated β-galactosidase, UUO unilateral ureteral obstruction.

staining showed that the SA-β-gal positive staining in the cytoplasm was also increased in MTEC after Ang-II treatment (Fig. 6h, i). These results suggested that cell senescence was exacerbated in renal tubular epithelial cells during kidney fibrosis.

Inhibition of Usp11 attenuated renal cell senescence in UUO mice
To explore the role of Usp11 and Tgfbr2 elevation of the senescence of fibrotic mouse kidney tissue, MTX was used to inhibit the effect of Usp11. Western blot results showed that MTX attenuated the changes in cell senescence-related gene expressions, such as the increase in γH2AX, P53, P21, and decrease in Klotho in UUO kidneys (Fig. 7a–c). SA-β-gal staining showed that MTX reduced the SA-β-gal positive staining area in UUO kidneys (Fig. 7d, e). These results suggested that the elevation of Usp11 and Tgfbr2 was implicated in cell senescence in UUO mice.

Interference of Usp11 alleviated Ang-II-induced activation on cell senescence-related Smad3/P53 pathway
To investigate the downstream pathway of Tgfbr2 regulated by USP11 in cell senescence, Western blot results showed that the phosphorylation of Smad3 was increased, and the expression of P53, P21, and P16 was also upregulated after Ang-II treatment. MTX attenuated the phosphorylation of Smad3 and blunted the expression of P53, P21, and P16 (Fig. 8a–c). Meanwhile, cell SA-β-gal staining showed that inhibition of Usp11 with MTX in MTECs attenuated the increase in SA-β-gal positive staining induced by Ang-II treatment (Fig. 8d, e). In the same time, knocked down on Usp11 in MTECs blunted the expression of cell senescence-related genes such as γH2AX, P53, and P21 after Ang-II treatment. The increase in SA-β-gal positive staining induced by Ang-II treatment was also partially reversed by knockdown on Usp11 (Fig. 8f–i). These results suggested that the elevation of Usp11 and Tgfbr2 facilitated cell senescence by activating Smad3/P53 signaling pathway.

DISCUSSION

Cell senescence is a state in which the cells gradually lose the endowed specific functions and proliferation ability. In multicellular organisms, cellular senescence is the cellular basis of

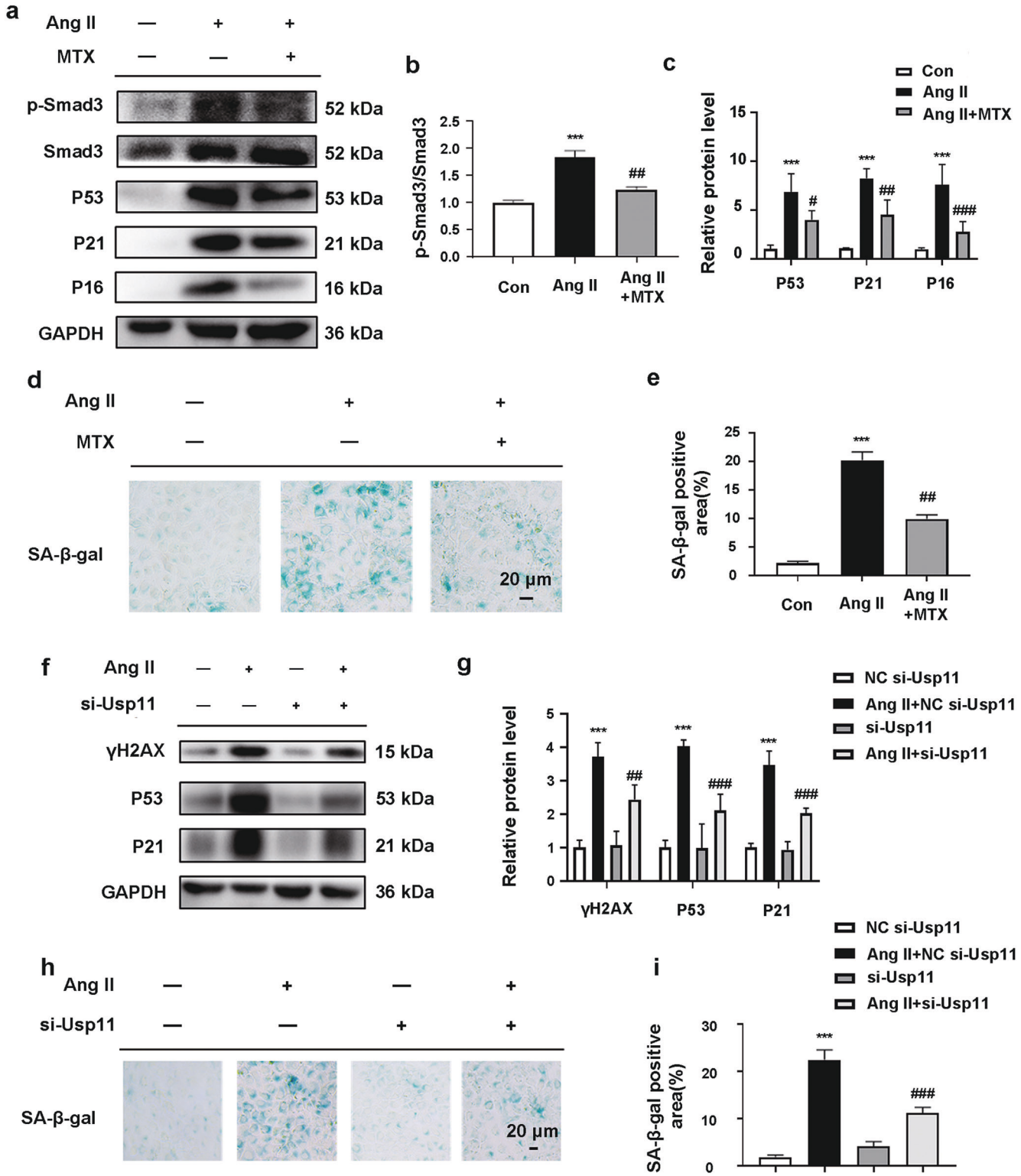

Fig. 8 Interference of Usp11 alleviated Ang-II-induced activation on cell senescence-related Smad3/P53 pathway. a Representative Western blot of p-Smad3, Smad3, P53, P21, and p16. Cells were pre-treated with Ang-II (10^{-6} M) for 48 h and then treated with MTX for 0.5 h. **b**, **c** Quantitative data for p-Smad3/Smad3, P53, P21 and p16 after Ang-II and MTX treatment ($n = 3$). $^{***}P < 0.001$ vs Con. $^{\#}P < 0.05$, $^{\#\#}P < 0.01$, $^{\#\#\#}P < 0.001$ vs Ang-II. **d**, **h** Representative SA-β-gal staining Images from different groups. Scale bars: 20 μm. **e**, **i** Quantitative determination of SA-β-gal positive area ($n = 3$). $^{***}P < 0.001$ vs Con. $^{\#\#}P < 0.01$ vs Ang-II. $^{***}P < 0.001$ vs NC si-Usp11. $^{\#\#\#}P < 0.001$ vs Ang-II + NC-Usp11. **f** Representative Western blot the levels of cell senescence markers in MTECs. **g** Quantitative data of cell senescence markers from different groups. $^{***}P < 0.001$ vs NC si-Usp11. $^{\#\#}P < 0.01$, $^{\#\#\#}P < 0.001$ vs Ang-II + NC-Usp11. Con control, MTX mitoxantrone, SA-β-gal Senescence-associated β-galactosidase, MTEC mouse tubular epithelial cell.

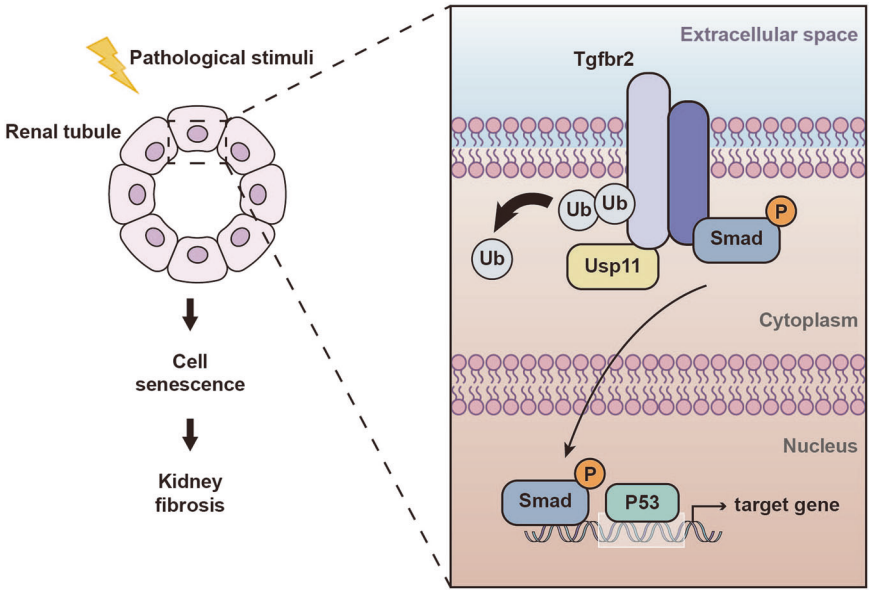

Fig. 9 The schematic diagram of Usp11 in promoting renal fibrosis. The expression of Usp11 is increased under pathological conditions, which prevents Tgfbr2 degradation via its deubiquitination effect. The elevation of Tgfbr2 promotes the over activation of downstream Smad3/P53 pathway, which induces tubular cell senescence and accelerates the renal fibrosis.

organismal ageing. Senescent cells are cell cycle arrested and cannot re-enter the cell cycle as required, which will ultimately impair the tissue renewal, and lead to functional deterioration. Senescent cells are characterized by morphological changes, chromosome DNA damage and chromatin remodeling, altered gene expressions, and the appearance of SASP [25, 30]. Recent studies have shown that various insults such as stress may result in accelerated cell senescence. As a consequence, the accelerated senescence will lead to tissue remodeling and functional degeneration. Therefore, accelerated senescence is recently considered as a reason for organ deterioration under pathological conditions, especially in chronic degenerative diseases. Revealing the relationship between cell senescence and injury is becoming a hot area in research for years to come [20, 31].

Studies have shown that CKD patients exhibit characteristics of a premature senescence syndrome, many factors that facilitate the development of CKD, including oxidative stress, persistent inflammation, are closely related to appearance of senescent phenotype and decreased klotho expression [25, 32, 33]. Senescent cells exhibit secretory phenotype, most of the cytokines secreted are pro-inflammatory cytokines, which can further promote the progression of renal fibrosis, thus accelerated cell senescence and inflammation form a vicious circle in promoting renal fibrosis [25, 31]. Kidney is a highly differentiated organ. Renal tubular cells, the most abundant terminally differentiated cells in kidney, are the cells most likely to transition into the senescent phenotype in CKD [34–37]. Studies have shown that the appearance of senescent phenotype of tubular epithelial cell is closely related to renal deterioration and fibrosis, but the upstream mechanism in triggering cell senescence is still unclear [24, 25, 38].

Available evidence showed that DNA damage response induced by sustained stress and telomere shortening may lead to the activation of p53. As a tumor suppressor, p53 is able to initiate the expression of p21, a cell cycle-associated protein which can lead to cell cycle arresting and appearance of senescent phenotype [39]. As an essential downstream signal molecule of TGF-β1, Smad3 is a transcriptional co-activator of p53, so the activation of TGF-β1 and the downstream signaling pathway will ultimately relate to cell cycle arresting and senescence [20]. Here, in UUO or FA-induced fibrotic mice, our results showed that the renal tubular epithelial cells presented senescent phenotype. Meanwhile, the Smad3/p53 signaling pathway was activated; in cultured mouse renal tubular epithelial cells, application of Ang-II, the key effector in RAS which facilitates renal fibrosis, also resulted in the appearance of cell senescence, these results suggest that tubular cell senescence is closely associated with renal fibrosis. In UUO or FA-induced fibrotic kidneys, the protein level of Tgfbr2 was elevated significantly and mainly distributed in renal epithelial cells. However, an interesting phenomenon observed in the experiment was that no significant elevation of the mRNA levels of Tgfbr2 was observed in fibrotic kidneys, so we speculated that the elevation of Tgfbr2 under pathological conditions might be affected by post-translational regulation.

UPS is one of the major post-translational regulatory systems of protein. Our results showed that as an important deubiquitinating enzyme, Usp11 was not only significantly increased in fibrotic kidneys, but also co-distributed with Tgfbr2 in renal tubular epithelial cells. Co-IP and IP results showed that Usp11 was able to interact with Tgfbr2 directly. The ubiquitination level of Tgfbr2 was decreased following Ang II treatment while knockdown on Usp11 was able to increase the ubiquitination level of Tgfbr2. These results suggested that the elevated Usp11 decreased the ubiquitination of Tgfbr2, and then resulted in the suppression in Tgfbr2 degradation, thus elevated Tgfbr2 protein level during renal fibrosis. After the inhibition of Usp11, the elevation of Tgfbr2 was significantly decreased, meanwhile, renal cell senescence and renal fibrosis were alleviated. These results confirmed that Usp11-related Tgfbr2 elevation was involved in renal senescence and fibrosis. Therefore, our study demonstrated that tubular cell senescence was altered during the progression of renal fibrosis, which was associated with the elevation of Usp11 and Tgfbr2. Pathological factors led to the elevation of Usp11, which decreased the ubiquitination of Tgfbr2 and increased its protein level, and then promoted cell senescence via activating the Smad3/P53 signaling pathway (Fig. 9).

Here, we identified that the elevations of Usp11 and Tgfbr2 were involved in renal cell senescence and the development and progression of renal fibrosis under pathological conditions. However, in our study, the upstream molecular mechanism in regulating USP11 elevation under pathological conditions had not been elucidated, also the E3 ubiquitin ligases that involved in the regulation of Tgfbr2 ubiquitination remained unknown. Although

our study demonstrated that elevated USP11 promoted renal tubular cell senescence and the progression of renal fibrosis via regulating Tgfbr2 under pathological conditions, it cannot be rule out that there are other mechanisms contributing to renal fibrosis by promoting renal parenchymal cell senescence.

In conclusion, our data demonstrated that pathological stimulation can increase the expression of Usp11 in renal tubular epithelial cells, which stabilizes Tgfbr2 and prevents its degradation by deubiquitination. The elevation of Tgfbr2 leads to persistent activation of the downstream Smad3/P53 pathway, and then promotes renal fibrosis through accelerating tubular senescence. Above all, inhibition of Usp11 may become one of the effective ways to protect against renal fibrosis.

ACKNOWLEDGEMENTS

This research was financially supported by the National Natural Science Foundation of China (82070712, 81873603) and the Science and Technology Commission of Shanghai Municipality (14DZ2260200, the project of Shanghai Key Laboratory of Kidney and Blood Purification).

AUTHOR CONTRIBUTIONS

LML, JL, JYN participated in the design of the study. LML, JYN, and XW wrote the paper. JYN and XW performed the experiments and analyzed the results. JYN, XW, HYX, NHY, JYL, XAS, HJG, LZ, and WZ took part in the revision of the manuscript.

ADDITIONAL INFORMATION

Competing interests: The authors declare no competing interests.

REFERENCES

1. Zhang L, Long J, Jiang W, Shi Y, He X, Zhou Z, et al. Trends in chronic kidney disease in China. N Engl J Med. 2016;375:905–6.
2. Saran R, Robinson B, Abbott KC, Bragg-Gresham J, Chen X, Gipson D, et al. US renal data system 2019 annual data report: epidemiology of kidney disease in the United States. Am J Kidney Dis. 2020;75:A6–a7.
3. Humphreys BD. Mechanisms of renal fibrosis. Annu Rev Physiol. 2018;80:309–26.
4. Ruiz-Ortega M, Rayego-Mateos S, Lamas S, Ortiz A, Rodrigues-Diez RR. Targeting the progression of chronic kidney disease. Nat Rev Nephrol. 2020;16:269–88.
5. Meng XM, Nikolic-Paterson DJ, Lan HY. TGF-β: the master regulator of fibrosis. Nat Rev Nephrol. 2016;12:325–38.
6. Vander Ark A, Cao J, Li X. TGF-β receptors: In and beyond TGF-β signaling. Cell Signal. 2018;52:112–20.
7. Liu S, Chen S, Zeng J. TGF-β signaling: a complex role in tumorigenesis (Review). Mol Med Rep. 2018;17:699–704.
8. Gifford CC, Tang J, Costello A, Khakoo NS, Nguyen TQ, Goldschmeding R, et al. Negative regulators of TGF-β1 signaling in renal fibrosis; pathological mechanisms and novel therapeutic opportunities. Clin Sci. 2021;135:275–303.
9. Wang W, Zhu Y, Sun Z, Jin C, Wang X. Positive feedback regulation between USP15 and ERK2 inhibits osteoarthritis progression through TGF-β/SMAD2 signaling. Arthritis Res Ther. 2021;23:84.
10. Zhang S, Xie C, Li H, Zhang K, Li J, Wang X, et al. Ubiquitin-specific protease 11 serves as a marker of poor prognosis and promotes metastasis in hepatocellular carcinoma. Lab Invest. 2018;98:883–94.
11. Tu L, Lin Z, Huang Q, Liu D. USP15 enhances the proliferation, migration, and collagen deposition of hypertrophic scar-derived fibroblasts by deubiquitinating TGF-βR1 in vitro. Plast Reconstr Surg. 2021;148:1040–51.
12. Zhang L, Zhou F, Drabsch Y, Gao R, Snaar-Jagalska BE, Mickanin C, et al. USP4 is regulated by AKT phosphorylation and directly deubiquitylates TGF-β type I receptor. Nat Cell Biol. 2012;14:717–26.
13. Bard JAM, Goodall EA, Greene ER, Jonsson E, Dong KC, Martin A. Structure and function of the 26S proteasome. Annu Rev Biochem. 2018;87:697–724.
14. Luza S, Opazo CM, Bousman CA, Pantelis C, Bush AI, Everall IP. The ubiquitin proteasome system and schizophrenia. Lancet Psychiatry. 2020;7:528–37.
15. Snyder NA, Silva GM. Deubiquitinating enzymes (DUBs): regulation, homeostasis, and oxidative stress response. J Biol Chem. 2021;297:101077.
16. Harrigan JA, Jacq X, Martin NM, Jackson SP. Deubiquitylating enzymes and drug discovery: emerging opportunities. Nat Rev Drug Discov. 2018;17:57–78.
17. Harper S, Gratton HE, Cornaciu I, Oberer M, Scott DJ, Emsley J, et al. Structure and catalytic regulatory function of ubiquitin specific protease 11 N-terminal and ubiquitin-like domains. Biochemistry. 2014;53:2966–78.
18. Jacko AM, Nan L, Li S, Tan J, Zhao J, Kass DJ, et al. De-ubiquitinating enzyme, USP11, promotes transforming growth factor β-1 signaling through stabilization of transforming growth factor β receptor II. Cell Death Dis. 2016;7:e2474.
19. Calcinotto A, Kohli J, Zagato E, Pellegrini L, Demaria M, Alimonti A. Cellular senescence: aging, cancer, and injury. Physiol Rev. 2019;99:1047–78.
20. Di Micco R, Krizhanovsky V, Baker D, d'Adda di Fagagna F. Cellular senescence in ageing: from mechanisms to therapeutic opportunities. Nat Rev Mol Cell Biol. 2021;22:75–95.
21. Gorgoulis V, Adams PD, Alimonti A, Bennett DC, Bischof O, Bishop C, et al. Cellular senescence: defining a path forward. Cell. 2019;179:813–27.
22. Hernandez-Segura A, Nehme J, Demaria M. Hallmarks of cellular senescence. Trends Cell Biol. 2018;28:436–53.
23. He S, Sharpless NE. Senescence in health and disease. Cell. 2017;169:1000–11.
24. Docherty MH, O'Sullivan ED, Bonventre JV, Ferenbach DA. Cellular senescence in the kidney. J Am Soc Nephrol. 2019;30:726–36.
25. Luo C, Zhou S, Zhou Z, Liu Y, Yang L, Liu J, et al. Wnt9a promotes renal fibrosis by accelerating cellular senescence in tubular epithelial cells. J Am Soc Nephrol. 2018;29:1238–56.
26. Miao NJ, Xie HY, Xu D, Yin JY, Wang YZ, Wang B, et al. Caspase-11 promotes renal fibrosis by stimulating IL-1β maturation via activating caspase-1. Acta Pharmacol Sin. 2019;40:790–800.
27. Reis-Mendes A, Dores-Sousa JL, Padrão AI, Duarte-Araújo M, Duarte JA, Seabra V, et al. Inflammation as a possible trigger for mitoxantrone-induced cardiotoxicity: an in vivo study in adult and infant mice. Pharmaceuticals. 2021;14:510.
28. Subramaniam V, Chuang G, Xia H, Burn B, Bradley J, Maderdrut JL, et al. Pituitary adenylate cyclase-activating polypeptide (PACAP) protects against mitoxantrone-induced cardiac injury in mice. Peptides. 2017;95:25–32.
29. Brandão SR, Reis-Mendes A, Domingues P, Duarte JA, Bastos ML, Carvalho F, et al. Exploring the aging effect of the anticancer drugs doxorubicin and mitoxantrone on cardiac mitochondrial proteome using a murine model. Toxicology. 2021;459:152852.
30. Chen JH, Hales CN, Ozanne SE. DNA damage, cellular senescence and organismal ageing: causal or correlative? Nucleic Acids Res. 2007;35:7417–28.
31. de Magalhães JP, Passos JF. Stress, cell senescence and organismal ageing. Mech Ageing Dev. 2018;170:2–9.
32. Stenvinkel P, Larsson TE. Chronic kidney disease: a clinical model of premature aging. Am J Kidney Dis. 2013;62:339–51.
33. Zhou L, Li Y, Zhou D, Tan RJ, Liu Y. Loss of Klotho contributes to kidney injury by derepression of Wnt/β-catenin signaling. J Am Soc Nephrol. 2013;24:771–85.
34. Verzola D, Gandolfo MT, Gaetani G, Ferraris A, Mangerini R, Ferrario F, et al. Accelerated senescence in the kidneys of patients with type 2 diabetic nephropathy. Am J Physiol Ren Physiol. 2008;295:F1563–73.
35. Zhu K, Kakehi T, Matsumoto M, Iwata K, Ibi M, Ohshima Y, et al. NADPH oxidase NOX1 is involved in activation of protein kinase C and premature senescence in early stage diabetic kidney. Free Radic Biol Med. 2015;83:21–30.
36. Sis B, Tasanarong A, Khoshjou F, Dadras F, Solez K, Halloran PF. Accelerated expression of senescence associated cell cycle inhibitor p16INK4A in kidneys with glomerular disease. Kidney Int. 2007;71:218–26.
37. Satriano J, Mansoury H, Deng A, Sharma K, Vallon V, Blantz RC, et al. Transition of kidney tubule cells to a senescent phenotype in early experimental diabetes. Am J Physiol Cell Physiol. 2010;299:C374–80.
38. Li C, Xie N, Li Y, Liu C, Hou FF, Wang J. N-acetylcysteine ameliorates cisplatin-induced renal senescence and renal interstitial fibrosis through sirtuin1 activation and p53 deacetylation. Free Radic Biol Med. 2019;130:512–27.
39. Hafner A, Bulyk ML, Jambhekar A, Lahav G. The multiple mechanisms that regulate p53 activity and cell fate. Nat Rev Mol Cell Biol. 2019;20:199–210.